Proceedings of DSCC2008
2008 ASME Dynamic Systems and Control Conference
October 20-22, 2008, Ann Arbor, Michigan, USA

DSCC2008-2262

DYNAMIC THRESHOLD METHOD BASED AIRCRAFT ENGINE SENSOR FAULT DIAGNOSIS

Wenfei Li, Rama K. Yedavalli
Department of Aerospace Engineering
The Ohio State University
Columbus, Ohio 43210
Email: li.537@osu.edu, yedavalli.1@osu.edu

ABSTRACT

It is challenging to have a good fault diagnostic scheme that can distinguish between model uncertainties and occurrence of faults, which helps in reducing false alarms and missed detections. In this paper, a dynamic threshold algorithm is developed for aircraft engine sensor fault diagnosis that accommodates parametric uncertainties. Using the robustness analysis of parametric uncertain systems, we generate upper-and-lower bound trajectories for the dynamic threshold. The extent of parametric uncertainties is assumed to be such that the perturbed eigenvalues reside in a set of distinct circular regions. Dedicated observer scheme is used for engine sensor fault diagnosis design. The residuals are errors between estimated state variables from a bank of Kalman filters. With this design approach, the residual crossing the upper-and-lower bounds of the dynamic threshold indicates the occurrence of fault. Application to an aircraft gas turbine engine Component Level Model clearly illustrates the improved performance of the proposed method.

NOMENCLATURE

CLM	Component Level Model
FDI	Fault Detection and Isolation
DOS	Dedicated Observer Scheme
HPC	High Pressure Compressor
HPT	High Pressure Turbine
LPC	Low Pressure Compressor
LPT	Low Pressure Turbine
WF36	Fuel flow
AE24	Variable bleed valve
STP25	Variable stator vane angle
XN2	Low pressure rotor speed sensor
XN25	High pressure rotor speed sensor
T49	LPT inlet temperature
TMHS23	Booster metal temperature
TMHS3	HPC metal temperature
TMHS41	HPT nozzle metal temperature
TMHS49	LPT metal temperature

INTRODUCTION

The demand for a safer and reliable aircraft gas turbine engine control system continues to grow rapidly. It has stimulated considerable research on aircraft gas turbine engine fault detection and isolation (FDI) approaches and technologies over decades. A real challenge in FDI application is the design of a scheme which can distinguish between model uncertainties and occurrence of faults. Therefore, it is important to design an approach to accommodate uncertainties in the model that would help in minimizing the false alarms and missed detections.

Currently, a threshold for aircraft engine FDI is usually predetermined and constant based on the empirical data. There are no useful guidelines for constant optimal threshold selections. Simani introduced a simple threshold detection methodology in [1] by using a state estimation approach. Lughofer et al used a threshold which is set to 3 or 4 times the accuracy of the corresponding sensor in [2]. An empirically trained fault detection threshold method was presented by Depold et al [3]. However, if a fixed threshold is set too high, it has reduced sensitivity to faults; if it is too low, false alarm rate increases. In case of large maneuvers and component degradation, it may happen that there is no fixed threshold that allows satisfactory FDI at a tol-

erable false alarm rate. Kobayashi and Simon also mentioned in [4] that a fixed threshold was not good enough to cover the range of an engine operation, although a constant threshold was still used in their papers [4–8]. In the absence of faults, a predetermined constant threshold would lead to more false alarms and missed detections under modeling uncertainties. Thus a dynamic threshold that is a function of time, control activity, and noise is a possible solution to the above problem. The basic idea of an adaptive threshold was elaborated in automobile applications in [9]. The notion of adaptive threshold is also discussed by Kobayashi in [4], but no details and no algorithms are presented. A preliminary version of this dynamic/adaptive threshold approach has been discussed by the authors in the paper [10].

The time response bounds for linear continuous-time parametric uncertain system was discussed by Yedavalli et al in [11]. Time response analysis of state variables is a standard means to study the transient and steady-state time-domain performance of a system. Parametric uncertainties introduce perturbations in the eigenvalues and eigenvectors, which alter the characteristics of a nominal system. The perturbed eigenvalue and eigenvector bounds greatly affect the upper-and-lower bounds on the perturbed state variables. The upper-and-lower bounds of a state variable generate a tube-shaped region around the nominal response. The time responses within this tube-shaped region guarantee the performance of the parametric uncertain system. In this paper, the methodology of generating a tube-shaped region for parametric uncertain systems developed in [11] is extended to the case of a linear discrete-time system. For the FDI logic, residuals are generated using a Dedicated Observer Scheme (DOS) and used in conjunction with the proposed dynamic threshold approach to detect faults in the presence of parametric uncertainties. Residuals are the errors between the state estimates from a set of Kalman filters. In the presence of a fault, the time response of residuals would cross either the lower bound or upper bound of the dynamic threshold. Thus this approach clearly distinguishes between the time response perturbations due to parametric uncertainties and the actual occurrence of faults. The paper is organized as follows: in the next section we discuss the sensor fault FDI scheme based on dedicated Kalman filter scheme. In a later section we discuss the dynamic threshold generation technique. Then we illustrate the application of this methodology to an aircraft gas turbine sensor fault diagnostics and offer some conclusions.

DEVELOPMENT OF AN AIRCRAFT SENSOR FAULT FDI SYSTEM

The design of a dynamic threshold with upper-and-lower bounds associated to the time response of the system is discussed in this paper. The Dedicated Observer Scheme in Figure 1 is used to detect and isolate faults through a bank of Kalman filters combined with the dynamic threshold. The aircraft engine FDI scheme is shown in Figure 2.

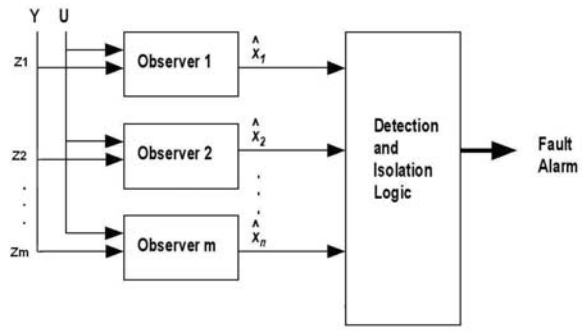

Figure 1. DEDICATED OBSERVER SCHEME

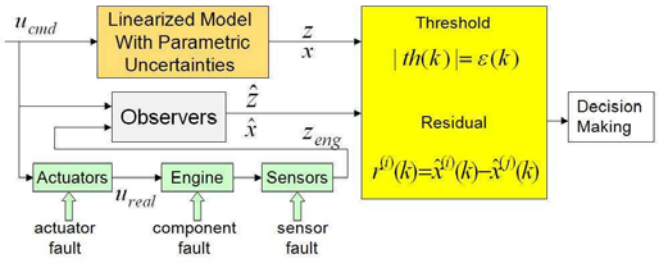

Figure 2. AIRCRAFT ENGINE FDI SCHEME

Engine System Model

The aircraft engine model with sensor fault can be modeled as

$$\begin{aligned} \dot{x}(t) &= f[x(t),u(t),t] + G(t)w(t) \\ z(t) &= h[x(t),u(t)] + v(t) + f(t) \end{aligned} \tag{1}$$

where $x(t) \in R^n$, $u(t) \in R^l$ and $z(t) \in R^m$ represent state variables, control command inputs, and sensor outputs. $w(t)$ is a set of white process noise with covariance Q, and $v(t)$ is a set of white sensor noise with covariance R. The nonlinear system can be linearized and discretized at different operating points. $f(t) \in R^m$ is the sensor fault representation. $f(t) = 0$ when there is no fault in the system. The linearized discretized model at one operating point associated with sensor faults is given by

$$\begin{aligned} x(k+1) &= \Phi x(k) + \Psi u(k) + w_d(k) \\ z(k+1) &= Hx(k+1) + Gu(k+1) + v(k+1) + f(k+1) \end{aligned} \tag{2}$$

where $w_d(k)$ is process noise with covariance Q_d, $v(k+1)$ is sensor noise with covariance R, and $f(k+1)$ is a sensor fault vector.

Kalman Filter Based Dedicated Observer Scheme FDI Design

Design a bank of Kalman filters to estimate the state variables and the output variables for the linearized discrete-time system.
In absence of faults:

$$\hat{x}^{(i)} = x \ \ for \ \ (i = 1,2,\cdots,n).$$

If sensor z_p is faulty:

$$\hat{x}^{(p)} \neq x \ \ and \ \ \hat{x}^{(i)} = x \ \ for \ \ (i = 1,2,\cdots,n \ \ and \ \ i \neq p).$$

DOS Using Kalman Filters. Decompose the output space as

$$\begin{aligned} z^{(1)}(k) &= H^{(1)}x(k) + G^{(1)}u(k) + v^{(1)}(k) + f^{(1)}(k) \\ &\vdots \\ z^{(m)}(k) &= H^{(m)}x(k) + G^{(m)}u(k) + v^{(m)}(k) + f^{(m)}(k) \end{aligned}$$

where $H = [H^{(1)},\cdots,H^{(m)}]'$, and $f = [f^{(1)},\cdots,f^{(m)}]'$. Design Kalman filters using each decomposed output. Assume $(\Phi, H^{(i)})$ pair is observable.

Kalman filter 1:
$\hat{x}^{(1)}(k|k) = \hat{x}^{(1)}(k|k-1) + K^{(1)}(k)[z^{(1)}(k) - \hat{z}^{(1)}(k|k-1)]$
$\vdots$
Kalman filter m:
$\hat{x}^{(m)}(k|k) = \hat{x}^{(m)}(k|k-1) + K^{(m)}(k)[z^{(m)}(k) - \hat{z}^{(m)}(k|k-1)]$

The residuals are defined by using the estimated states.

$$\begin{aligned} r^{(1)} &= \hat{x}^{(1)} - \hat{x}^{(2)} \\ r^{(2)} &= \hat{x}^{(2)} - \hat{x}^{(3)} \\ &\vdots \\ r^{(m)} &= \hat{x}^{(m)} - \hat{x}^{(1)} \end{aligned}$$

The FDI decision making logic is given in Table 1, for $m = 3$ case.

DYNAMIC THRESHOLD DESIGN USING TIME RESPONSE BOUNDS FOR LINEAR DISCRETE-TIME PARAMETRIC UNCERTAIN SYSTEM

Assume the nominal linear discrete-time system model is represented as,

$$\begin{aligned} x(k+1) &= \Phi x(k) + \Psi u(k) \\ z(k+1) &= Hx(k+1) + Gu(k+1) \end{aligned} \tag{3}$$

where $x(0) = x_0$, $x(k) \in R^n$, $u(k) \in R^l$ and $z(k) \in R^m$ represent state variables, control command inputs, and measured sensor outputs. Assume the system is stable, i.e. all the eigenvalues fall in the unit circle in z-domain. The solution to system (3) is given by

$$x(k) = \Phi^k x_0 + \sum_{j=0}^{k-1} \Phi^{k-1-j} B u(j) \tag{4}$$

The perturbed system with real parametric uncertainties is represented as

$$\begin{aligned} x_e(k+1) &= (\Phi + E)x_e(k) + \Psi u(k) \\ z_e(k+1) &= Hx_e(k+1) + Gu(k+1) \end{aligned} \tag{5}$$

where $x_e(0) = x_0$, $x_e(k) \in R^n$ and $z_e(k) \in R^m$ represent state variables and sensor outputs under uncertainties, $E \in R^{n \times n}$ represents the parametric uncertainty matrix. The solution to the system (5) is given by

$$x_e(k) = (\Phi + E)^k x_0 + \sum_{j=0}^{k-1} (\Phi + E)^{k-1-j} B u(j) \tag{6}$$

Assume that Φ has distinct eigenvalues spectrum $(\lambda_1, \lambda_2, ..., \lambda_n)$, and $(\Phi + E)$ has distinct eigenvalues spectrum $(\mu_1, \mu_2, ..., \mu_n)$. If V is a modal matrix diagonalizing Φ, then

$$\Phi = V \Lambda V^{-1} = V \Lambda W \tag{7}$$

where

$$W = \begin{bmatrix} w_1 \\ w_2 \\ \vdots \\ w_n \end{bmatrix}, \ \ V = \begin{bmatrix} v_1 \ v_2 \ \cdots \ v_n \end{bmatrix}$$

and

$$\Lambda = \begin{bmatrix} \lambda_1 & & & \\ & \lambda_2 & & \\ & & \ddots & \\ & & & \lambda_n \end{bmatrix} = diag(\lambda_1, \lambda_2, \cdots, \lambda_n)$$

where w_i is a row vector, v_i is a column vector, $i = 1, 2, \ldots, n$, then

$$\Phi v_j = \lambda_j v_j \text{ and } w_j \Phi = \lambda_j w_j.$$

Table 1. FDI Decision Making

Fault in Sensor#1	Fault in Sensor#2	Fault in Sensor#3
$r^{(1)}$ crosses threshold	$r^{(1)}$ crosses threshold	$r^{(1)} = 0$
$r^{(2)} = 0$	$r^{(2)}$ crosses threshold	$r^{(2)}$ crosses threshold
$r^{(3)}$ crosses threshold	$r^{(3)} = 0$	$r^{(3)}$ crosses threshold

If V_e is a modal matrix diagonalizing $(\Phi + E)$, then

$$\Phi + E = V_e \Lambda_e V_e^{-1} = V_e \Lambda_e W_e \tag{8}$$

where

$$W_e = \begin{bmatrix} w_{e_1} \\ w_{e_2} \\ \vdots \\ w_{e_n} \end{bmatrix}, \quad V_e = \begin{bmatrix} v_{e_1} & v_{e_2} & \cdots & v_{e_n} \end{bmatrix}$$

and

$$\Lambda_e = \begin{bmatrix} \mu_1 & & & \\ & \mu_2 & & \\ & & \ddots & \\ & & & \mu_n \end{bmatrix} = diag(\mu_1, \mu_2, \cdots, \mu_n)$$

then

$$\mu_j = \lambda_j + \vec{\rho}_{jj}; \quad v_{e_j} = v_j + \Delta v_j; \quad w_{e_j} = w_j + \Delta w_j$$

$$(\Phi + E) v_{e_j} = \mu_j v_{e_j} \text{ and } w_{e_j} (\Phi + E) = \mu_j w_{e_j}.$$

where $\vec{\rho}_{jj}$ is the perturbation of the j-th eigenvalue, Δv_j and Δw_j are the perturbations of the j-th eigenvectors. Then the time-response of the m-th element of nominal state variable vector $x(k)$ can be written as:

$$x_m(k) = \sum_{i=1}^{n} v_{m_i} \lambda_i^k w_i x_0 + \sum_{j=0}^{k-1} \sum_{i=1}^{n} v_{m_i} \lambda_i^{k-1-j} w_i B u(j) \tag{9}$$

The time-response of the m-th element of perturbed state variable vector $x_e(k)$ can be written as:

$$\begin{aligned} x_{e_m}(k) = & \sum_{i=1}^{n} (v_{m_i} + \Delta v_{m_i}) \mu_i^k w_{e_i} x_0 \\ & + \sum_{j=0}^{k-1} \sum_{i=1}^{n} (v_{m_i} + \Delta v_{m_i}) \mu_i^{k-1-j} w_{e_i} B u(j) \end{aligned} \tag{10}$$

where $(\cdot)_m$ refers to the m-th element of a column vector $(\cdot)$; and $(\cdot)_{m_i}$ refers to the m-th element of a column vector $(\cdot)_i$.

Time Response Analysis

Because of the existence of the parametric uncertainties in the system, the eigenvalues and eigenvectors are different from the nominal system. We assume that the nominal eigenvalues are distinct, and the perturbed eigenvalues lie in disjointed domains (no overlaps among each domain). An example of the distinct eigenvalue distribution and the corresponding eigenvalue and eigenstructure (including the effect of eigenvectors) perturbation regions are shown in Figure (3). Define

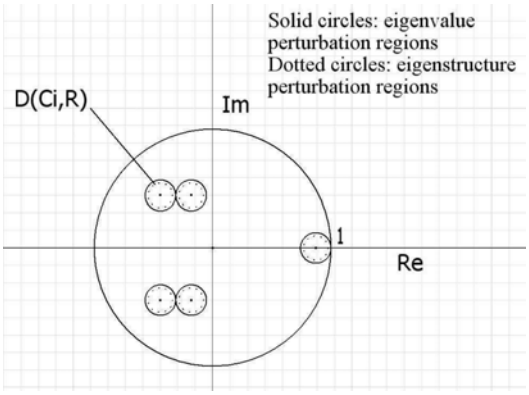

Figure 3. AN EXAMPLE OF DISJOINTED DOMAIN

$$x_m^0(k) = \sum_{i=1}^{n} v_{m_i} \lambda_i^k w_i x_0 \tag{11}$$

$$x_m^u(k) = \sum_{j=0}^{k-1} \sum_{i=1}^{n} v_{m_i} \lambda_i^{k-1-j} w_i B u(j) \tag{12}$$

$$x_{e_m}^0(k) = \sum_{i=1}^{n} (v_{m_i} + \Delta v_{m_i}) \mu_i^k w_{e_i} x_0 \tag{13}$$

$$x_{e_m}^u(k) = \sum_{j=0}^{k-1} \sum_{i=1}^{n} (v_{m_i} + \Delta v_{m_i}) \mu_i^{k-1-j} w_{e_i} B u(j) \tag{14}$$

where $x_m^0(k)$ and $x_m^u(k)$ are the zero-input time response and zero-state time response for the nominal system (3) respectively; $x_{e_m}^0(k)$ and $x_{e_m}^u(k)$ are the zero-input time response and zero-state

time response for the perturbed system (5) respectively. Then

$$x_m(k) = x_m^0(k) + x_m^u(k)$$
$$x_{e_m}(k) = x_{e_m}^0(k) + x_{e_m}^u(k)$$

The time response of the bound between the perturbed state variable and the nominal state variable is

$$\begin{aligned} |x_{e_m}(k) - x_m(k)| &\le |x_{e_m}^0(k) - x_m^0(k)| + |x_{e_m}^u(k) - x_m^u(k)| \\ &= \varepsilon_m^0(k) + \varepsilon_m^u(k) = \varepsilon_m(k) \end{aligned} \tag{15}$$

Zero-Input Response Bound. The time response of Equation (13) can be written as

$$x_{e_m}^0(k) = \sum_{i=1}^{n} \{v_{m_i}\mu_i^k w_i + v_{m_i}\mu_i^k \Delta w_i + \Delta v_{m_i}\mu_i^k w_{e_i}\} x_0 \tag{16}$$

then the difference of the zero-input time response between the perturbed system (5) and the nominal system (3) is

$$\begin{aligned} x_{e_m}^0(k) - x_m^0(k) = \sum_{i=1}^{n} \{ & v_{m_i}(\mu_i^k - \lambda_i^k) w_i + v_{m_i}\mu_i^k \Delta w_i \\ & + \Delta v_{m_i}\mu_i^k w_{e_i}\} x_0 \end{aligned} \tag{17}$$

So the bound of the zero-input response is

$$\begin{aligned} |x_{e_m}^0(k) - x_m^0(k)| \le \sum_{i=1}^{n} \{ & |v_{m_i}||\mu_i^k - \lambda_i^k|\|w_i\| + |v_{m_i}||\mu_i^k|\|\Delta w_i\| \\ & + |\Delta v_{m_i}||\mu_i^k|\|w_{e_i}\|\}\|x_0\| \end{aligned} \tag{18}$$

The details of the bounds for the perturbations of the eigenvectors and eigenvalues were proved in paper [11], while the results of those bounds are used in this paper,

$$\|w_i\| = \pi_i, \quad \|v_i\| = \delta_i, \quad \|\Delta w_i\| \le \frac{R_\theta \pi_i}{\alpha_i - R_\theta},$$

$$\|\Delta v_{m_i}\| \le \|\Delta v_i\| \le \frac{R_\theta \delta_i}{\alpha_i - R_\theta}, \quad \|w_{e_i}\| = \|w_i + \Delta w_i\| \le \frac{\pi_i \alpha_i}{\alpha_i - R_\theta},$$

where $\alpha_i = \sigma_{\max}(\Phi - \lambda_i I)$, $R_\theta \le \frac{\mathcal{K}(V)}{\mathcal{K}(V)+1} R_{\min}$, where $\mathcal{K}(V)$ is the condition number for the modal matrix V, $R_{\min}$ is the minimum radius for the disjointed domain. Also it can be proved

$$\begin{aligned} |\mu_i^k - \lambda_i^k| &= |(\lambda_i + \vec{\rho}_{ii})^k - \lambda_i^k| \\ &= |\lambda_i|^k \left| \sum_{j=0}^{k} \binom{k}{j} \left(\frac{\vec{\rho}_{ii}}{\lambda_i}\right)^j - 1 \right| \\ &= |\lambda_i|^k \left| \sum_{j=1}^{k} \binom{k}{j} \left(\frac{\vec{\rho}_{ii}}{\lambda_i}\right)^j \right| \\ &\le |\lambda_i|^k \sum_{j=1}^{k} \binom{k}{j} \left|\frac{\vec{\rho}_{ii}}{\lambda_i}\right|^j \\ &\le |\lambda_i|^k \sum_{j=1}^{k} \binom{k}{j} \left(\frac{R_\theta}{|\lambda_i|}\right)^j \\ &\le |\lambda_i|^k \left[\left(1 + \frac{R_\theta}{|\lambda_i|}\right)^k - 1 \right] \end{aligned} \tag{19}$$

Similarly,

$$|\mu_i^k| \le |\lambda_i|^k \left(1 + \frac{R_\theta}{|\lambda_i|}\right)^k \tag{20}$$

Substitute the above bounds into the function (18), the zero-input bound can be obtained by

$$\begin{aligned} |x_{e_m}^0(k) - x_m^0(k)| \le \sum_{i=1}^{n} |\lambda_i|^k \{ & \left(1 + \frac{R_\theta}{|\lambda_i|}\right)^k [\frac{|v_{m_i}|\pi_i \alpha_i}{\alpha_i - R_\theta} \\ & + \frac{R_\theta \delta_i \pi_i \alpha_i}{(\alpha_i - R_\theta)^2}] - |v_{m_i}|\pi_i\} \|x_0\| = \varepsilon_m^0(k) \end{aligned} \tag{21}$$

Zero-State Response Bound. The time response of Equation (14) can be written as

$$\begin{aligned} x_{e_m}^u(k) = \sum_{j=0}^{k-1} \sum_{i=1}^{n} [& v_{m_i}\mu_i^{k-1-j} w_i + v_{m_i}\mu_i^{k-1-j} \Delta w_i \\ & + \Delta v_{m_i}\mu_i^{k-1-j}(w_i + \Delta w_i)] B u(j) \end{aligned} \tag{22}$$

then the difference of the zero-state time response between the perturbed system (5) and the nominal system (3) is

$$\begin{aligned} x_{e_m}^u(k) - x_m^u(k) = \sum_{j=0}^{k-1} \sum_{i=1}^{n} [& v_{m_i}(\mu_i^{k-1-j} - \lambda_i^{k-1-j}) w_i \\ & + v_{m_i}\mu_i^{k-1-j} \Delta w_i \\ & + \Delta v_{m_i}\mu_i^{k-1-j}(w_i + \Delta w_i)] B u(j) \end{aligned} \tag{23}$$

So the zero-state response bound is

$$|x^u_{e_m}(k) - x^u_m(k)| \leq \sigma_{\max}(B) \sum_{j=0}^{k-1} \sum_{i=1}^{n} |\lambda_i|^{k-1-j} \{ \left(1 + \frac{R_\theta}{|\lambda_i|}\right)^{k-1-j} \cdot \left[\frac{|v_{m_i}|\alpha_i\pi_i}{\alpha_i - R_\theta} + \frac{R_\theta \delta_i \pi_i \alpha_i}{(\alpha_i - R_\theta)^2} \right] - |v_{m_i}|\pi_i \} \|u(j)\| = \varepsilon^u_m(k) \quad (24)$$

Hence the time response bound between the perturbed state variable and the nominal state variable is obtained as

$$|x_{e_m}(k) - x_m(k)| \leq \varepsilon^0_m(k) + \varepsilon^u_m(k) = \varepsilon_m(k) \quad (25)$$

The dynamic threshold is given by

$$|th^{(m)}(k)| = \varepsilon_m(k) \quad (26)$$

APPLICATION OF DYNAMIC THRESHOLD APPROACH TO AIRCRAFT GAS TURBINE ENGINE

The algorithms described in the previous sections are applied for a linear discrete-time model of an aircraft engine. The real engine model is a highly nonlinear continuous-time model. Thus linearization and discretization of the engine model is performed. In this section, a description of the aircraft engine model is given.

Aircraft Engine Simulation Model

The aircraft engine model used in this paper is a nonlinear simulation model of an advanced high-bypass two-spool turbofan engine. It has been developed as a Component Level Model (CLM), which contains the major components of an aircraft engine, such as Fan or Low Pressure Compressor (LPC), High Pressure Compressor (HPC), High Pressure Turbine (HPT) and Low Pressure Turbine (LPT). The CLM characterizes highly complex engine dynamics and simulates real-time data. Six state variables, three control inputs and three sensors are used in this study, and are shown in Table 2. A similar engine model has also been studied in [12] and [13]. In this paper the engine is simulated from stillness to idle under non-deteriorated condition.

Simulation Results

Assume the control command is zero. The nonlinear engine model is linearized and discretized by setting a sampling time $T = 0.2$sec. The time response bounds for each of the six state variables are calculated. The initial condition is set as $x_0 = [5,\ 5,\ 2,\ 1,\ 1,\ 1]'$.

Let us inject a bias fault in sensor #2 (XN25). The corresponding diagnostic result is shown in Figure 4. The residuals cross the tube-shaped dynamic thresholds which is consistent with the logic in Table 1, indicating a fault in sensor #2.

Table 2. STATE VARIABLES, ACTUATORS, AND SENSORS

State Variables	Actuators	Sensors
XN2, XN25	WF36	XN2
TMHS23, TMHS3	AE24	XN25
TMHS41, TMHS49	STP25	T49

The dynamic threshold approach involves the inner dynamics of the engine system and it gives the upper-and-lower bounds of the time response under parametric uncertainties, hence it is dynamically changing and following the behavior of the system in absence of faults. A constant threshold is not good enough for an engine fault diagnosis as mentioned in the previous section, irrespective of whether it is selected to be a large or small value. Usually the constant threshold is chosen based on experimental data and knowledge of the physical phenomenon. It does not follow the dynamics of the system due to large maneuvers, control activity and outside disturbances. The dynamic threshold eliminates the inaccuracy or inconsistency associated with the constant threshold approach.

CONCLUSIONS

An FDI scheme for an aircraft engine with dynamic threshold approach is presented in this paper. The dynamic threshold is designed based on an engine model with parametric uncertainties. This technique helps the system accommodate uncertainties in the model and reduce false alarms and missed detections. The algorithm presented here involves the condition number of the modal matrix of the system. It assumes that the system has a well-conditioned modal matrix since a nominal matrix with ill-conditioned modal matrix has no tolerance to parametric uncertainties. This is the conservative side of this methodology. Only a zero-input response of the engine system fault diagnosis is discussed in the paper. Efforts are under way to expand this method to include control input response.

REFERENCES

[1] Simani, S., 2005. "Identification and Fault Diagnosis of A Simulated Model of an Industrial Gas Turbine". *IEEE Transaction on Industrial Informatics,* **1**(3), August, pp. 202–216.

[2] Lughofer, E., Efendic, H., Re, L. D., and Klement, E. P., 2003. "Filtering of Dynamic Measurements in Intelligent Sensors for Fault Detection Based on Data-Driven Models". 42nd IEEE Conference on Decision and Control, pp. 463–468.

[3] Depold, H. R., Rajamani, R., Morrison, W. H., and Pattipati, K. R., 2006. "A Unified Metric for Fault Detection and Isolation in Engines". ASME paper No. GT2006-91095.

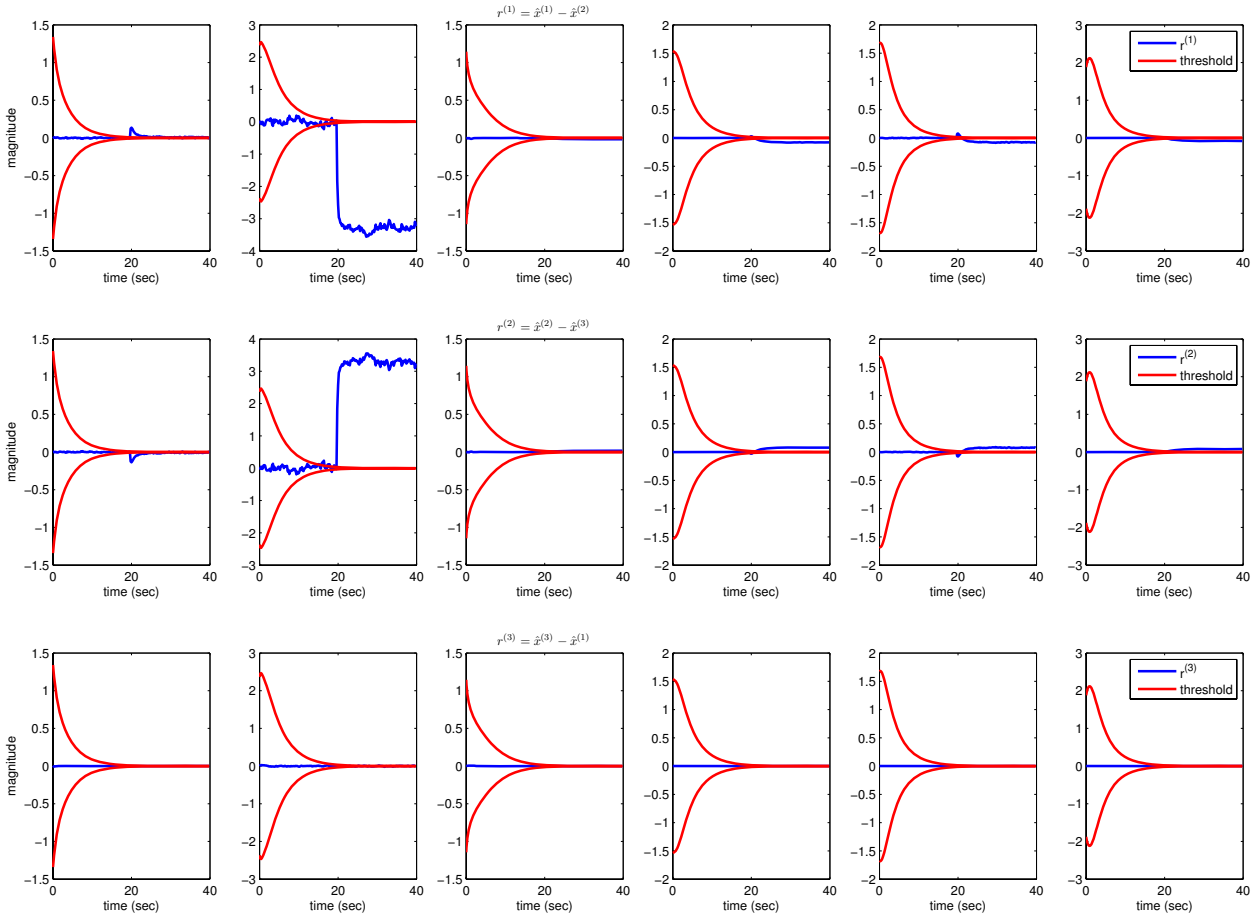

Figure 4. SENSOR XN25 FDI

[4] Kobayashi, T., and Simon, D. L., 2006. "Hybrid Kalman Filter Approach For aircraft engine in-flight diagnostics: sensor fault detection case". ASME paper No. GT2006-90870.

[5] Kobayashi, T., and Simon, D. L., 2007. "Integration of on-line and off-line diagnostic algorightms for aircraft engine health management". ASME paper No. GT2007-27518.

[6] Kobayashi, T., and Simon, D. L., 2003. "Application of a Bank of Kalman Filters for Aircraft Engine Fault Diagnostics". ASME paper No. GT2003-38550.

[7] Kobayashi, T., and Simon, D. L., 2004. "Evaluation of an Enhanced Bank of Kalman Filters for In-Flight Aircraft Engine Sensor Fault Diagnostics". ASME paper No. GT2004-53640.

[8] Kobayashi, T., Simon, D. L., and Litt, J. S., 2005. "Application of a Constant Gain Extended Kalman Filter for In-flight Estimation of Aircraft Engine Performance Parameters". ASME paper No. GT2005-68494.

[9] Pisu, P., Serrani, A., You, S., and Jalics, L. "Adaptive Threshold Based Diagnostics for Steer-By-Wire Systems". *ASME Journal of Dynamic Systems, Measurement, and Control,* **128**(2), pp. 428–435.

[10] Yedavalli, R. K., and Li, W., 2007. "Aircraft engine fault detection using dynamic/adaptive threshold approach". ASME TURBO EXPO GT2007-28180. Paper number GT2007-28180.

[11] Yedavalli, R. K., and Ashukkumar, C. R. "Time response bounds for linear parametric uncertain systems". *International Journal of Systems Science,* **31**(2), pp. 177–188.

[12] Shankar, P., and Yedavalli, R. K., 2006. "A Neural Network Based Adaptive Observer for Turbine Engine Parameter Estimation". ASME paper No.GT2006-90603.

[13] Litt, J. S., 2005. "An Optimal Orthogonal Decomposition Method for Kalman Filter-Based Turbofan Engine Thrust Estimation ". ASME paper No. GT2005-68808.